

~~RESTRICTED~~

UNCLASSIFIED
CLASSIFICATION CHANGED

To RESTRICTED

C.2

~~11354~~

By authority of *H. L. Dryden*

~~RESTRICTED~~
NACA

*per NACA Release form 724
dated 2-28-52
By HQR, 4-8-52. ADP*

RESEARCH MEMORANDUM

Authority *J. W. Crowley* Date *11/10/53*

By *DATA 124/53* See *Index*
rel. form # 158A

TESTS OF A HORIZONTAL-TAIL MODEL THROUGH
THE TRANSONIC SPEED RANGE BY THE
NACA WING-FLOW METHOD

By

Richard E. Adams and Norman S. Silsby
Langley Memorial Aeronautical Laboratory
Langley Field, Va.

CLASSIFIED DOCUMENT

This document contains classified information affecting the National Defense of the United States within the meaning of the Espionage Act, USC 50-81 and 82. Its transmission or the revelation of its contents in any manner to an unauthorized person is prohibited by law. Information so classified may be imparted only to persons in the military and naval services of the United States, appropriate civilian officers and employees of the Federal Government who have a legitimate interest therein, and to United States citizens of known loyalty and discretion who of necessity must be informed thereof.

NATIONAL ADVISORY COMMITTEE FOR AERONAUTICS

WASHINGTON

April 11, 1947

NACA LIBRARY
LANGLEY MEMORIAL AERONAUTICAL
LABORATORY
Langley Field, Va.

UNCLASSIFIED

~~RESTRICTED~~

By authority of
Date

To

CLASSIFICATION CHANGED

CLASSIFICATION CHANGED

To

Date
By authority of



CLASSIFIED

NATIONAL ADVISORY COMMITTEE FOR AERONAUTICS

RESEARCH MEMORANDUM

TESTS OF A HORIZONTAL-TAIL MODEL THROUGH
THE TRANSONIC SPEED RANGE BY THE
NACA WING-FLOW METHOD

By Richard E. Adams and Norman S. Silsby

SUMMARY

A $\frac{1}{12}$ -scale semispan model of a horizontal tail of a fighter airplane was tested at transonic speeds in the high-speed flow over an airplane wing, the surface of which served as a reflection plane for the model. Measurements of lift, elevator hinge moment, angle of attack, and elevator angle were made in the Mach number range from 0.75 to 1.04 for elevator deflections ranging from 10° to -10° and for angles of attack of -1.2° , 0.4° , and 3.4° . The equipment used to measure the hinge moments of the model proved to be rather unsatisfactory, and for this reason the hinge-moment data are considered to be only qualitative.

The results of the tests indicated that the elevator effectiveness, in general, decreased as the Mach numbers increased from 0.80 to 0.95. At all three angles of attack the effectiveness became zero or reversed over an elevator-deflection range of about 4° at Mach numbers around 0.95. The center of this ineffective range of elevator deflections δ_e varied with angle of attack α from positive elevator deflections at negative angles of attack to negative elevator deflections at positive angles of attack. The elevator, however, had regained appreciable effectiveness when sonic velocity was reached for all elevator deflections, and at a Mach number of 1.04 the mean elevator effectiveness $(dC_L/d\delta_e)_m$ was about 60 percent of the value at a Mach number of 0.75. The lift-curve slope $(dC_L/d\alpha)_m$ for angles of attack from 1.2° to 3.4° decreased about 40 percent as the Mach number increased from 0.75 to 0.93. With further increase in Mach number to 1.04, the slope increased to about the same value it had at a Mach number of 0.75. The hinge-moment data, which are considered to be qualitative only, indicated that the elevator became strongly overbalanced at Mach numbers between 0.91 and 0.96 and that this overbalance disappeared before sonic velocity was attained. The slope of the hinge-moment

curves became very steep at a Mach number of 1.04, at which the slope was about three times as large as the average slope at a Mach number of 0.75.

INTRODUCTION

In an effort to anticipate any difficulties that might be experienced with a full-scale airplane in high-speed dives a preliminary study of compressibility effects has been made at the Langley Memorial Aeronautical Laboratory of the NACA. Some information about the problem of stability and control at high Mach numbers has been determined for a semispan model of an airplane as presented in reference 1. The present tests were made to determine the elevator effectiveness and the hinge-moment characteristics of a $\frac{1}{12}$ -scale half-span model of a horizontal tail of a fighter airplane at high Mach numbers by the NACA wing-flow method. (See reference 2.)

Because of the urgent need for this information, existing equipment designed for measurement of lift, drag, and pitching moment of airfoils was modified to measure the control characteristics of the model. Numerous difficulties were encountered in the use of this equipment, especially for the determination of elevator hinge moments. Some information on the effectiveness of the control and some qualitative indications of the change of hinge-moment characteristics with Mach number were obtained, however, and are considered to be of general interest, particularly because the tests covered the speed range including sonic velocity. Measurements of lift and elevator hinge moments were made for elevator deflections ranging from -10° to 10° with angles of attack of -1.2° , 0.4° , and 3.4° and covered a range of Mach numbers from 0.74 to 1.05.

SYMBOLS

The following symbols apply to the model mounted on the airplane wing:

- α angle of attack
- t tail thickness
- c tail chord

~~CONFIDENTIAL~~

δ_e	deflection of elevator
c_e	elevator chord, behind hinge line
\bar{c}_e	root-mean-square chord of elevator, behind hinge line
x	distance along chord from leading edge
y	ordinate of section profile
S	area of semispan tail
S_e	area of semispan elevator, behind hinge line
$(t/c)_m$	mean thickness chord ratio
$(c_e/c)_m$	mean ratio of elevator chord to tail chord
H	hinge moment of elevator
L	lift
q	effective dynamic pressure of flow over model
M	effective Mach number of flow over model
R	Reynolds number based on mean aerodynamic chord of 3.36 inches
A	aspect ratio
C_L	lift coefficient (L/qS)
C_{H_e}	elevator hinge-moment coefficient ($H/q\bar{b}c_e^2$)
$(dC_L/d\delta_e)_m$	mean elevator effectiveness (change in C_L divided by change in δ_e over given range of δ_e)
$(dC_L/d\alpha)_m$	mean stabilizer effectiveness (change in C_L divided by change in α for given range of α)

The following symbols refer to the airplane on which the model was mounted:

x_a	chordwise distance along surface of airplane wing.
z_a	distance normal to surface of airplane wing

q_{x_a}	local dynamic pressure near surface of airplane wing at distance x_a along surface
M_{x_a}	local Mach number near surface of airplane wing at distance x_a along surface
C_{L_a}	airplane lift coefficient
M_o	flight Mach number
P_o	free-stream static pressure

APPARATUS, METHOD, AND TESTS

The tests were made by the NACA wing-flow method of reference 2, in which the model is mounted in the region of high-speed flow over the wing of an airplane. A P-51D airplane was used for the tests.

The semispan model was mounted over the ammunition-compartment door of the airplane, as shown in figures 1 and 2. The model, which was cut from brass, had the following geometric characteristics:

Tail:

Area, S (semispan), square inches	19.6
Root chord of tail, inches	4.12
Tip chord of tail, inches	2.28
Mean aerodynamic chord, inches	3.36
Semispan, inches	6.25
Taper ratio	1.81:1
Aspect ratio (wing surface considered as reflection plane)	3.99

Elevator:

Area, S_e (semispan), square inches	7.42
Chord at root, inches	1.42
Chord at tip, inch	0.73
Root-mean-square chord, inches	1.09

Profiles of sections of the model measured at three spanwise stations are compared in figure 3 with the design profiles. Measured ordinates of the tail are given in table I. Errors of construction resulted in a slight displacement of the elevator hinge axis from the chord line toward the upper surface as shown in figure 3. The size of the gap between the stabilizer and elevator, which was unsealed, was not measured directly but is indicated approximately on the profiles of figure 3 for the no-load condition. Because

of bending of the elevator with the application of lift loads, the gaps and the elevator hinge-axis location probably varied somewhat during the tests.

A circular end plate with a cut-out to provide for movement of the elevator was attached to the root of the stabilizer as shown in figures 1 and 2. A smaller plate was secured to the root of the elevator to minimize the flow of air through the cut-out in the main end plate.

The shank of the model passed through the ammunition-compartment door and was mounted on a balance arranged to measure lift force and elevator hinge moments. The balance arrangement was an adaptation of existing equipment designed for measurement of lift, drag, and pitching moments of airfoils and proved to be rather unsatisfactory for determination of hinge moments. Consequently, there is some uncertainty as to the accuracy of the hinge-moment data obtained. Provisions were made to measure the angle of the elevator as it oscillated through a range of angles from -10° to 10° at a rate of 18° per second, which for the full-scale airplane would correspond to $1\frac{1}{2}^{\circ}$ per second. The stabilizer was fixed at a given angle for each flight. The accuracy of the elevator angles is of the order of $\pm 0.1^{\circ}$, whereas the accuracy of the stabilizer angle is approximately $\pm 0.2^{\circ}$.

The direction of local air flow was determined by use of a free-floating vane of wedge-shape cross section mounted 22.5 inches outboard of the model station. (See fig. 2.) Oscillation of the elevator had no measurable effect on the direction of air flow at the vane; hence, there was probably no appreciable interaction. The direction of the local air flow at the model station relative to the flow direction at the reference vane was determined in a test with a similar vane arrangement mounted at the model station, as shown in figure 4.

The relation of Mach number of the local air flow close to the wing surface to the flight Mach number and to the airplane lift coefficient was established from pressure measurements with static-pressure orifices flush with the wing surface in tests before the model was mounted on the ammunition-compartment door. The contour of the door has been modified since the tests of reference 2 to cause formation of shock at a more rearward chordwise position and thereby to prevent the passage of shock over the model. Typical chordwise distributions of Mach number over the test region are shown in figure 5 for several flight Mach numbers M_0 and airplane lift coefficients C_{L_e} . Because of the chordwise variation in dynamic

pressure and Mach number over the wing surface at the model station, the values \bar{q} and \bar{M} used in the evaluation and presentation of the data were determined according to the relations:

$$\bar{q} = \frac{0.97}{S} \iint q_{x_a} dx_a dz_a$$

$$\bar{M} = \frac{0.97}{S} \iint M_{x_a} dx_a dz_a$$

where the integrals were taken over the area occupied by the model and $dx_a dz_a$ represents an element of this area. The factor 0.97 which takes approximate account of the decrease in the induced velocity with distance from the wing surface was determined from an incomplete investigation of the variation of static pressure with distance from the wing surface. The variations of \bar{q}/p_0 and \bar{M} with C_{L_a} were established from tests with the model off and were considered to apply for the tests with the model in place. The effects of the pressure gradients in the test region on the model characteristics are not known. The effect of the wing boundary layer on the model test results is believed to be small since unpublished flight data obtained at high speeds on a P-51 airplane wing indicate that the boundary-layer thickness at the model test station would be only about 3 or 4 percent of the model span.

Tests were made with angles of attack of -1.2° , 0.4° , and 3.4° and with elevator deflections from -10° to 10° . The measurements were made in high-speed dives from an altitude of 28,000 feet to 22,000 feet. The effective Mach numbers \bar{M} of the flow at the model station ranged from 0.75 to 1.04 and the Reynolds numbers R from 0.6×10^6 to 0.84×10^6 . The variation of Reynolds number with Mach number for the tests with various stabilizer settings is shown in figure 6. In the tests simultaneous photographic records were obtained of the elevator angle of the model, the angle of the reference vane, lift force of the model, hinge-moment of the elevator of the model, free-stream static pressure, free-stream impact pressure, and normal acceleration of the airplane.

PRESENTATION OF RESULTS

The results of the tests, covering the range of Mach numbers from 0.75 to 1.04, are presented in figures 7 to 11. The variation of lift coefficient C_L with effective Mach number \bar{M} for various

elevator deflections at each of the angles of attack of -1.2° , 0.4° , and 3.4° are shown in figure 7. The curves of figure 7 were obtained by cross-plotting time histories of C_L , δ_e , α , and M . The variation of lift coefficient with elevator deflection is presented in figure 8 for the three angles of attack and for various Mach numbers. The mean rate of change of the lift coefficient with elevator deflection $(dC_L/d\delta_e)_m$ for elevator deflections from 0° to -4° and from 0° to 4° are plotted in figure 9 against effective Mach number for the three angles of attack. The mean rate of change of lift coefficient with angle of attack $(dC_L/d\alpha)_m$ over the range from -1.2° to 3.4° is plotted against Mach number in figure 10 for elevator neutral. Because of the previously mentioned difficulties in obtaining elevator hinge-moment data with the equipment used for these tests, hinge-moment coefficients were determined only for the angle of attack of 0.4° over the elevator deflection range from -10° to 3° . These results, which are considered to be qualitative only, are presented in figure 11 as plots of hinge-moment coefficient against elevator deflection for various Mach numbers. These curves also were obtained by cross-plotting time histories of the observed data.

Values of $(dC_L/d\alpha)_m$ and $(dC_L/d\delta_e)_m$ from the tests in the Langley 8-foot high-speed tunnel of a model of the horizontal tail of a typical high-speed bomber (reference 3) are plotted against Mach number in figure 12 for comparison with results from the present tests of the tail model. The lift-curve slopes $(dC_L/d\alpha)_m$ were taken for the elevator-neutral condition and over the range of angle of attack of 1° to -1° for the tunnel tests and for the range of angle of attack of -1.2° to 3.4° for the wing-flow tests. The slopes $(dC_L/d\delta_e)_m$ were taken for $\alpha = 0^\circ$ and over the elevator-deflection range of 1° to -1° for the tunnel tests and for the angle of attack of 0.4° over the elevator-deflection range of 4° to -4° for the wing-flow tests.

DISCUSSION OF RESULTS

The results presented in figure 7 indicate that serious losses in lift of the model for given angles of attack and elevator deflection did not occur until a Mach number of at least 0.80 was attained. At higher Mach numbers the most marked change in the lift characteristics of the model was in the effectiveness of the elevator which, for part of the deflection range (depending on the angle of attack), became zero and reversed at Mach numbers of 0.90 to 1.00. (See fig. 7.) The complete loss or reversal of the control effectiveness generally

occurred over a range of elevator angles of about 3° or 4° as shown in figure 8; the center of this range varied from about 1° at an angle of attack of -1.2° to about -3° at an angle of attack of 3.4° . The asymmetry of the curves of figure 8 is probably due partly to the dissymmetry of the model elevator and is probably indicative of the unsymmetrical variations of elevator effectiveness that may be encountered in flight due to aerodynamic distortion of the control surfaces and possible manufacturing errors. The large influence of the angle of attack of the effectiveness of the elevator at Mach numbers approaching 1.0 is further illustrated in figure 9. For the elevator deflection range from 0° to 4° the value of $(dC_L/d\delta_e)_m$ at Mach numbers near 0.95 was almost zero for the 0.4° angle-of-attack condition and was negative for an angle of attack of -1.2° whereas, for an angle of attack of 3.4° , the loss in elevator effectiveness was relatively moderate over the Mach number range. With the elevator deflected from 0° to -4° , however, the value of $(dC_L/d\delta_e)_m$ for an angle of attack of 3.4° decreased rapidly at Mach numbers beyond 0.80 and became negative at Mach numbers near 0.95. The elevator effectiveness for an angle of attack of 0.4° was also reversed at Mach numbers around 0.95 for this elevator-deflection range, but with an angle of attack of -1.2° some effectiveness was maintained through this critical Mach number range. At sonic velocity positive elevator effectiveness had been regained for all conditions and at a Mach number of 1.04 the variation of lift coefficient with elevator deflection was almost linear throughout the deflection range. (See fig. 8(g).) For this Mach number the values of $dC_L/d\delta_e$ for the deflection range from -4° to 4° averaged about 60 percent of the values obtained at a Mach number of 0.75. Tests of a half span model of an airplane at transonic speeds, reported in reference 1, also indicated a total loss in elevator effectiveness at Mach numbers near 0.93 and a recovery of positive elevator effectiveness at a Mach number of unity.

The average lift-curve slope of the model $dC_L/d\alpha$ over the angle-of-attack range from -1.2° to 3.4° , elevator neutral (fig. 10), decreased from 0.066 at a Mach number of 0.75 to a minimum of 0.039 at a Mach number of 0.93. At Mach numbers of 1.0 and 1.04 the lift-curve slope had approximately the same value as at a Mach number of 0.75.

The slope of the curves of elevator hinge-moment coefficient against elevator deflection shown in figure 11 tended to become flatter over the deflection range from 0° to -6° as the Mach number was increased from 0.75 to 0.91. The elevator became strongly overbalanced at a Mach number of 0.96, which was about the same value at which the greatest loss in effectiveness of the elevator occurred. At this Mach number the elevator had a stable floating position at -8° which was undoubtedly determined to some extent by the dissymmetry of the model

caused by construction errors. (See fig. 3.) The slopes of the hinge-moment curve were very steep at the floating position and at the unstable zero hinge-moment position, which suggests that it would be very difficult to hold the elevator of the full-scale airplane at other than the floating positions by manual control. As the Mach number was increased from 0.96 to 1.00, the overbalance disappeared and at a Mach number of 1.04 the variation of hinge-moment coefficient with deflection was almost linear throughout the deflection range with a slope at least three times as great as the average slope at a Mach number of 0.75. Although difficulties encountered in the measurement of the hinge moments indicate that the quantitative values are subject to some error, the data are believed to be sufficiently correct to determine the general shapes and trends of the curves.

Results of tests in the Langley 8-foot high-speed tunnel of a model of the tail of a high-speed bomber (reference 3) showed a rapid decrease in elevator effectiveness, as represented by $(dC_L/d\delta_e)_m$, at Mach numbers above 0.85 similar to that obtained in the present tests of the tail model. (See fig. 12.) The tunnel tests also indicated, as did the present tests, that the loss in effectiveness of the stabilizer, represented by $(dC_L/d\alpha)_m$, at supercritical speeds, although substantial, was much less severe than the loss in elevator effectiveness. The differences in the absolute values of the effectiveness of the stabilizer and elevator from the tunnel tests and from the present tests is probably largely due to the differences in the thickness-chord ratio of the two models and to the fact that the tests of the bomber-tail model were made with a sealed elevator, whereas the elevator of the tail model of a fighter airplane was unsealed. Other possible sources of differences are the different chordwise velocity gradients in the flow fields about the models, the different Reynolds numbers, and the differences in the boundary conditions of the flow for the two test methods.

CONCLUSIONS

The results of the tests on a $\frac{1}{12}$ -scale, semispan model of a horizontal tail of a fighter airplane indicated that:

1. The elevator effectiveness in general decreased as the Mach number increased from 0.80 to 0.95. At all three angles of attack (-1.2° , 0.4° , and 3.4°) the effectiveness became zero or reversed over an elevator-deflection range of about 4° at Mach numbers around 0.95. The center of this ineffective range of elevator deflections varied with angle of attack from positive elevator deflections at negative angles of attack to negative elevator deflections at positive angles of attack. The elevator, however, had regained appreciable effectiveness by the

time sonic velocity was reached for all elevator deflections, and at a Mach number of 1.04 the mean elevator effectiveness $(dC_L/d\delta_e)_m$ was about 60 percent of the value at a Mach number of 0.75.

2. The lift-curve slope dC_L/da for angles of attack from -1.2° to 3.4° decreased about 40 percent as the Mach number increased from 0.75 to 0.93. With further increase in Mach number to 1.04 the slope increased to about the same value it had at a Mach number of 0.75.

3. The hinge-moment data, which are considered to be qualitative only, indicated that the elevator became strongly overbalanced at Mach numbers between 0.91 and 0.96 and that this overbalance disappeared before sonic velocity was attained. The slope of the hinge-moment curve became very steep at a Mach number of 1.04 at which the slope was about three times as large as the average slope at a Mach number of 0.75.

Langley Memorial Aeronautical Laboratory
National Advisory Committee for Aeronautics
Langley Field, Va.

REFERENCES

1. Zalovecik, John A., and Sawyer, Richard H.: Longitudinal Stability and Control Characteristics of a Half-Span Airplane Model at Transonic Speeds from Tests by the NACA Wing-Flow Method. NACA ACR No. L6F15, 1946.
2. Gilruth, R. R., and Wetmore, J. W.: Preliminary Tests of Several Airfoil Models in the Transonic Speed Range. NACA ACR No. L5E08, 1945.
3. Bielat, Ralph P.: Investigation at High Speeds of a Horizontal-Tail Model in the Langley 8-Foot High-Speed Tunnel. NACA RM No. L6F10b, 1947.

TABLE I

HORIZONTAL TAIL ORDINATES

MEASURED FROM MODEL

[Stations and ordinates in percent chord]

Station y	Ordinate			
	Root (a)		Tip (b)	
	Upper surface	Lower surface	Upper surface	Lower surface
0	0	0	0	0
1.25	1.32	-1.12	1.23	-1.11
2.5	1.96	-1.71	1.75	-1.62
5.0	2.87	-2.68	2.54	-2.41
7.5	3.52	-3.36	3.13	-3.01
10	3.95	-3.84	3.56	-3.46
15	4.57	-4.47	4.11	-4.10
20	4.87	-4.82	4.50	-4.54
25	4.98	-4.95	4.69	-4.74
30	4.95	-5.02	4.73	-4.80
40	4.62	-4.81	4.56	-4.66
50	4.02	-4.31	4.15	-4.11
60	3.30	-3.70	3.75	-3.95
65	2.75	-3.27	3.51	-3.58
70	3.34	-3.75	3.58	-4.05
75	3.32	-3.62	3.60	-4.13
80	2.94	-3.12	3.31	-3.67
85	2.26	-2.36	2.70	-2.96
90	1.48	-1.51	1.93	-2.12
95	.71	-.62	1.13	-1.12
100	0	0	0	0

^aMeasured 0.55 inch outboard of end plate.

^bMeasured 5.75 inches outboard of end plate.

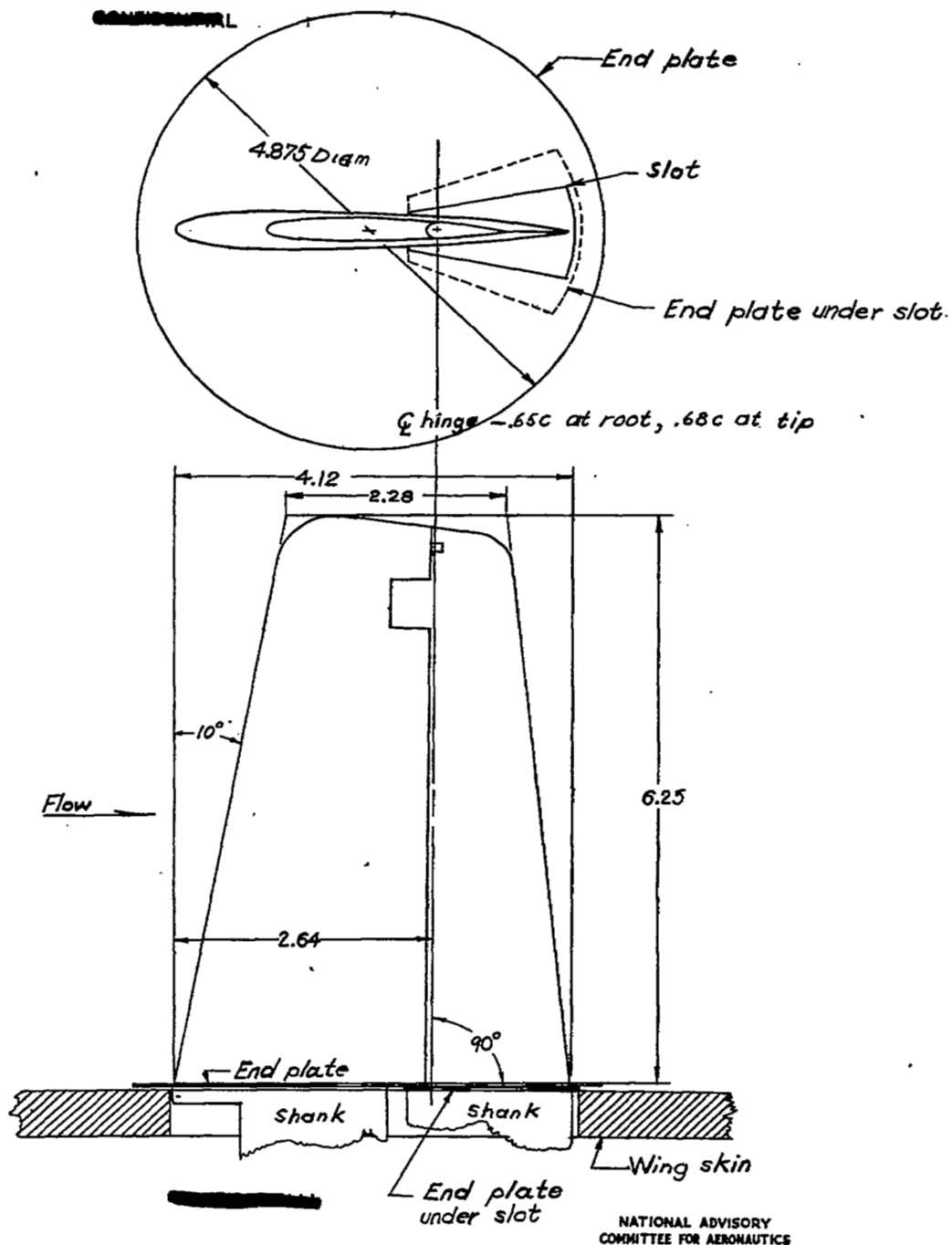


Figure 1.- Sketch of $\frac{1}{12}$ -scale, semispan model of the horizontal tail of a fighter airplane. (All dimensions are in inches.)

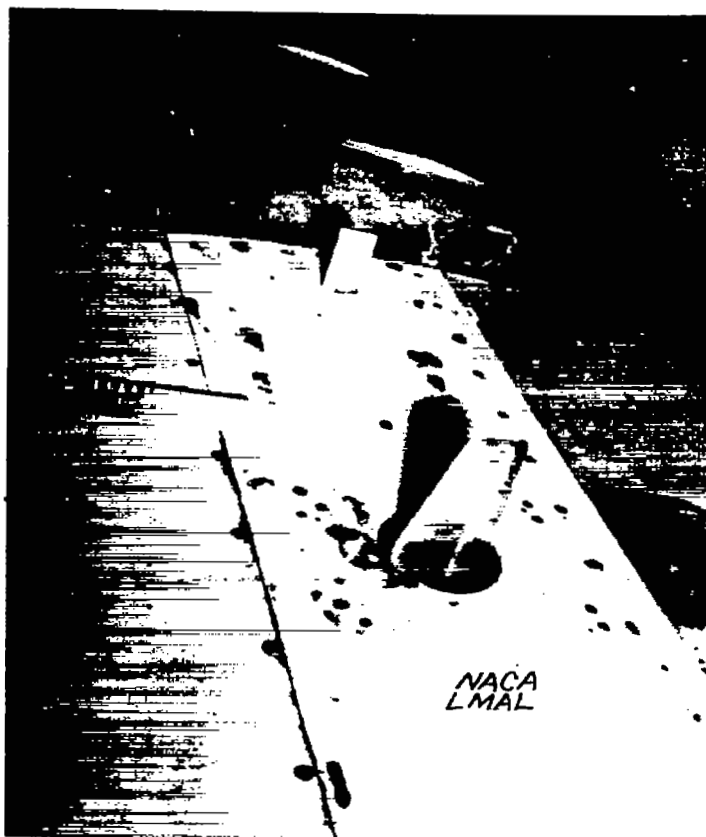


Figure 2.- Semispan $\frac{1}{12}$ -scale model of horizontal tail of a fighter airplane mounted over ammunition-compartment door of airplane wing. Reference vane mounted outboard of model.

00

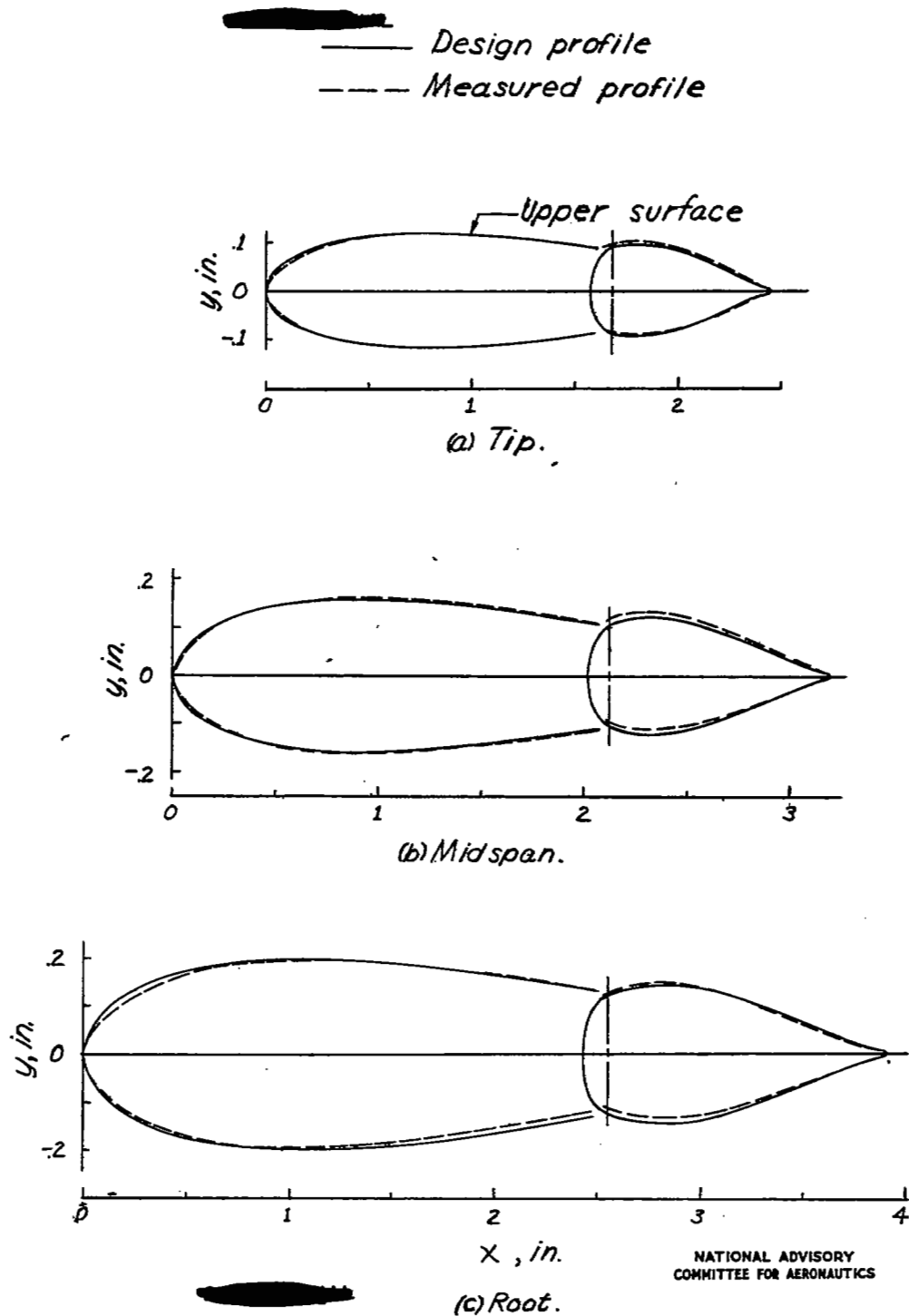


Figure 3.- Comparison of measured ordinates with design ordinates. The chordwise location of the elevator hinge axis is shown by the vertical broken lines. Angle of attack and elevator deflection taken as positive for clockwise rotation of the surfaces. (Ordinate scale 2.5 times abscissa scale.)

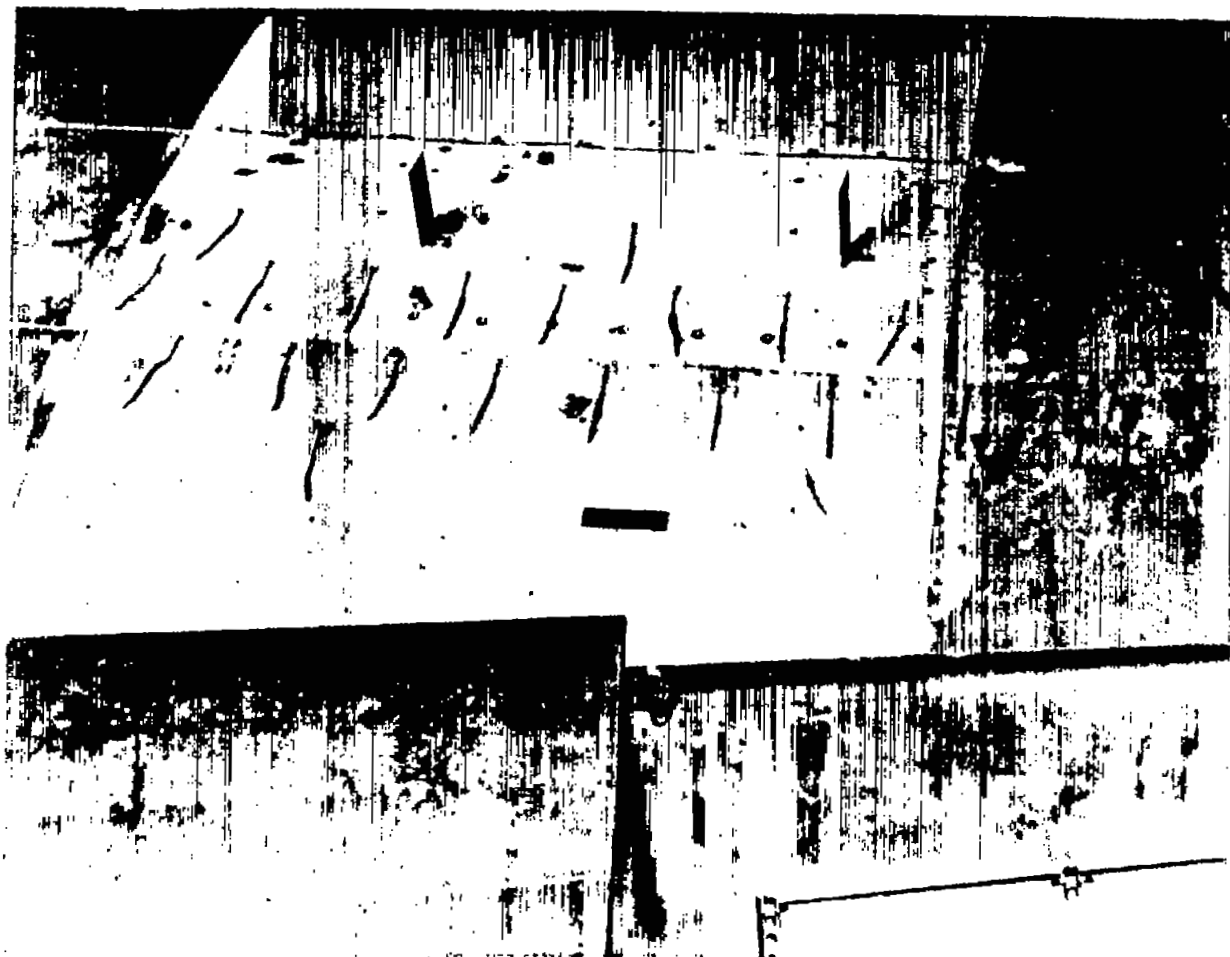
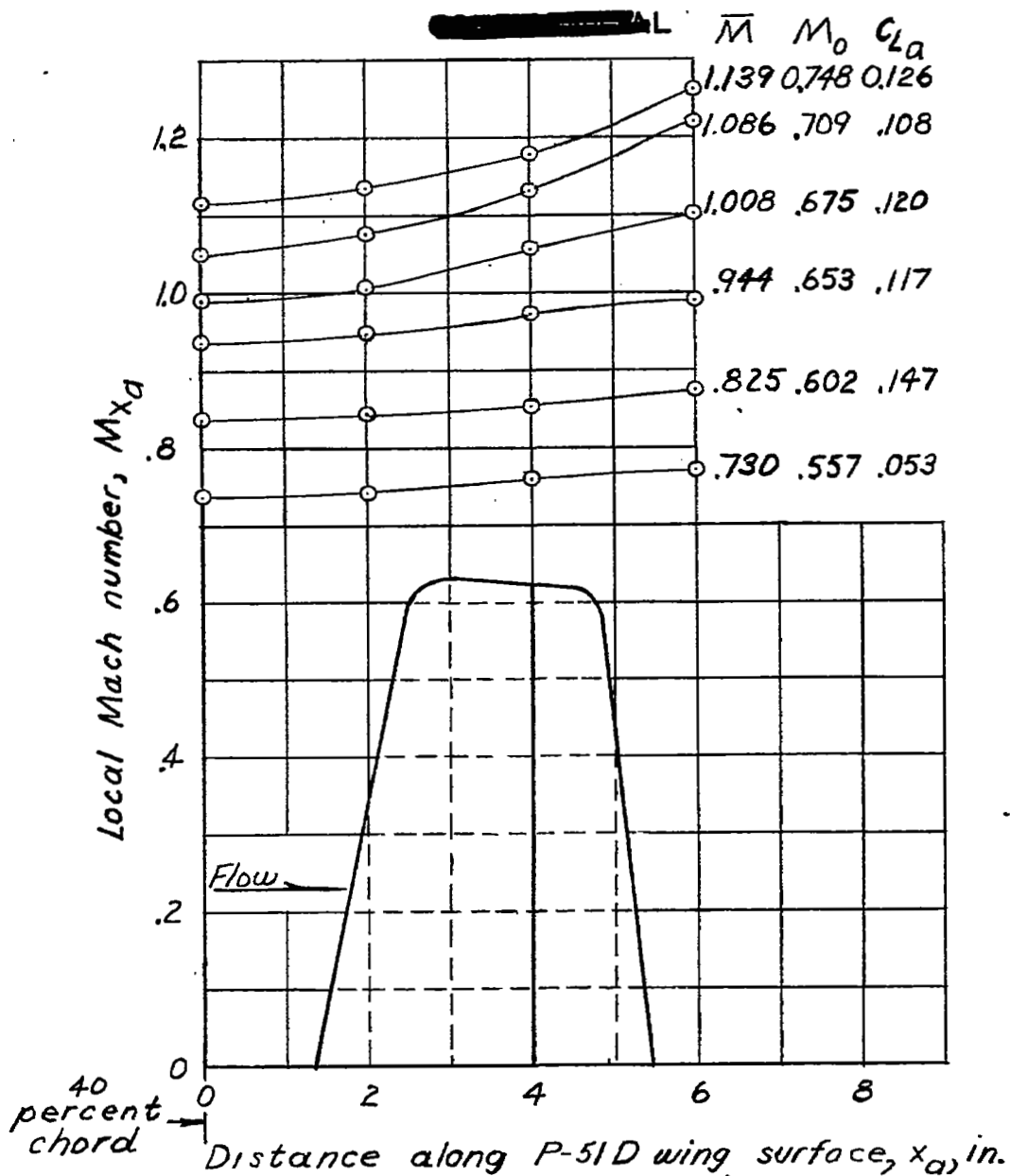


Figure 4.- Arrangement of free-floating vanes for determination of flow direction at model station.



NATIONAL ADVISORY
COMMITTEE FOR AERONAUTICS

Figure 5.- Typical chordwise distributions of Mach number over airplane wing in test region with model off for several flight Mach numbers M_0 and airplane lift coefficients C_{L_a} . Sketch below curve shows chordwise position of model on wing surface.

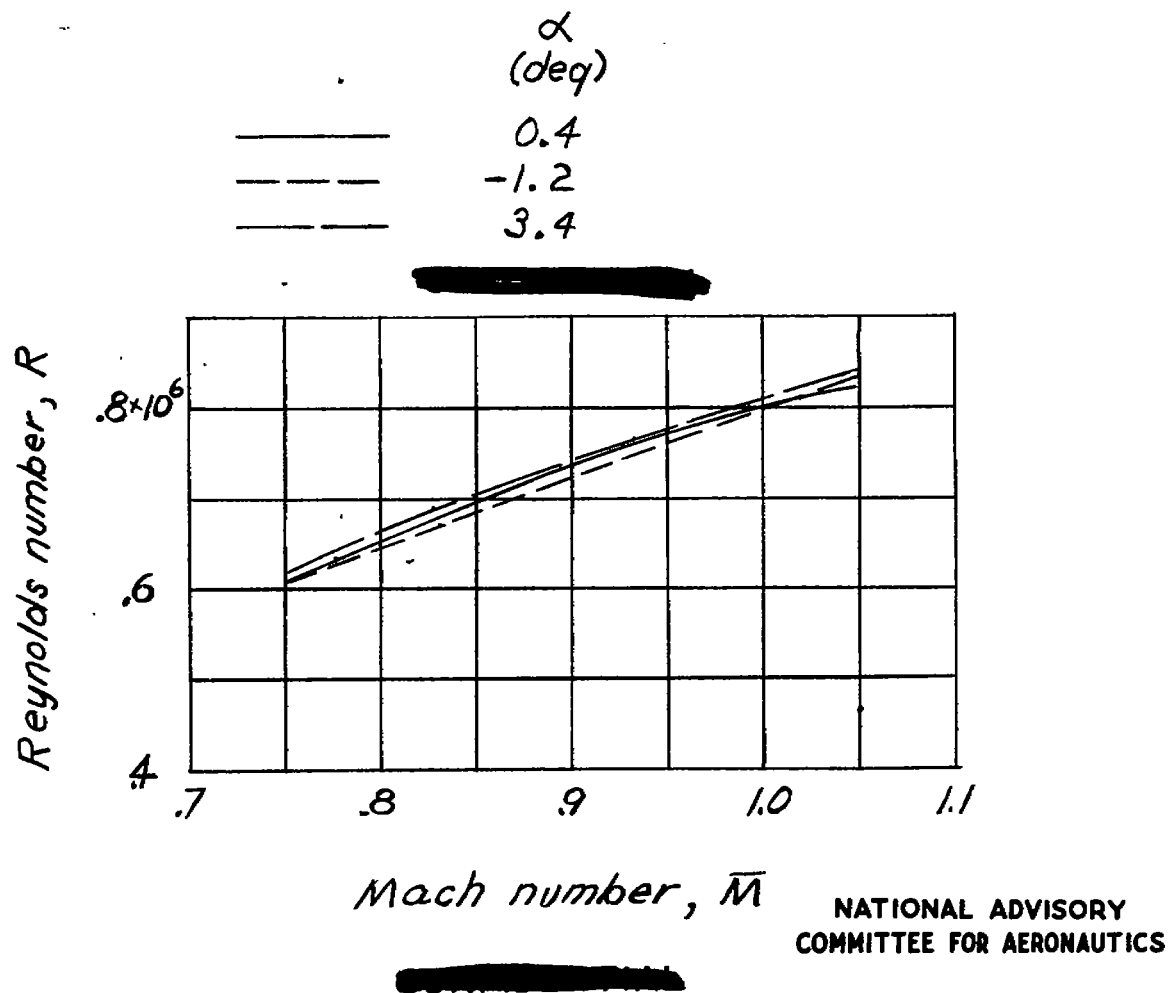


Figure 6.- Variation of Reynolds number with Mach number.

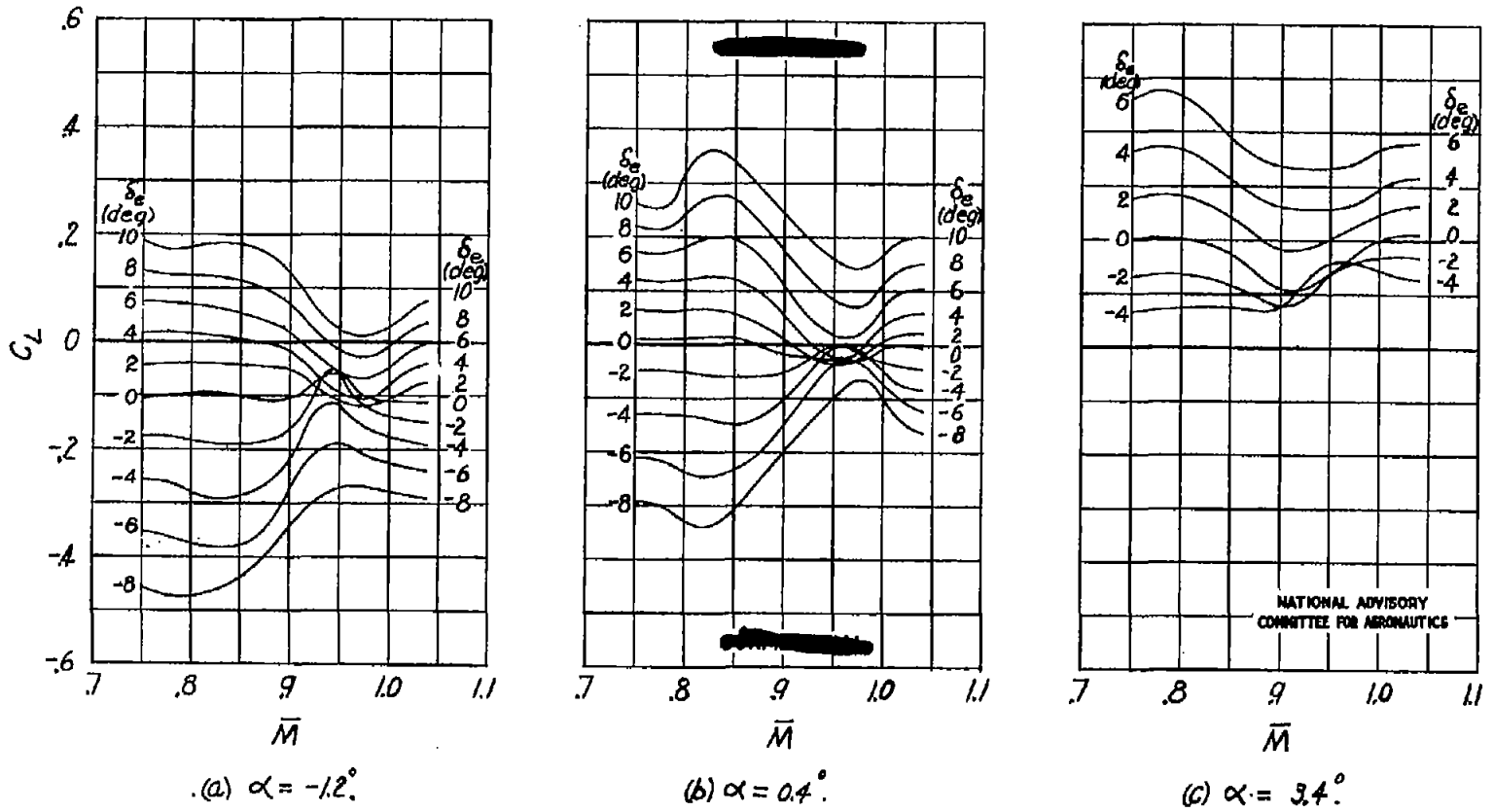


Figure 7.- Variation of lift coefficient with Mach number for several elevator deflections and angles of attack.

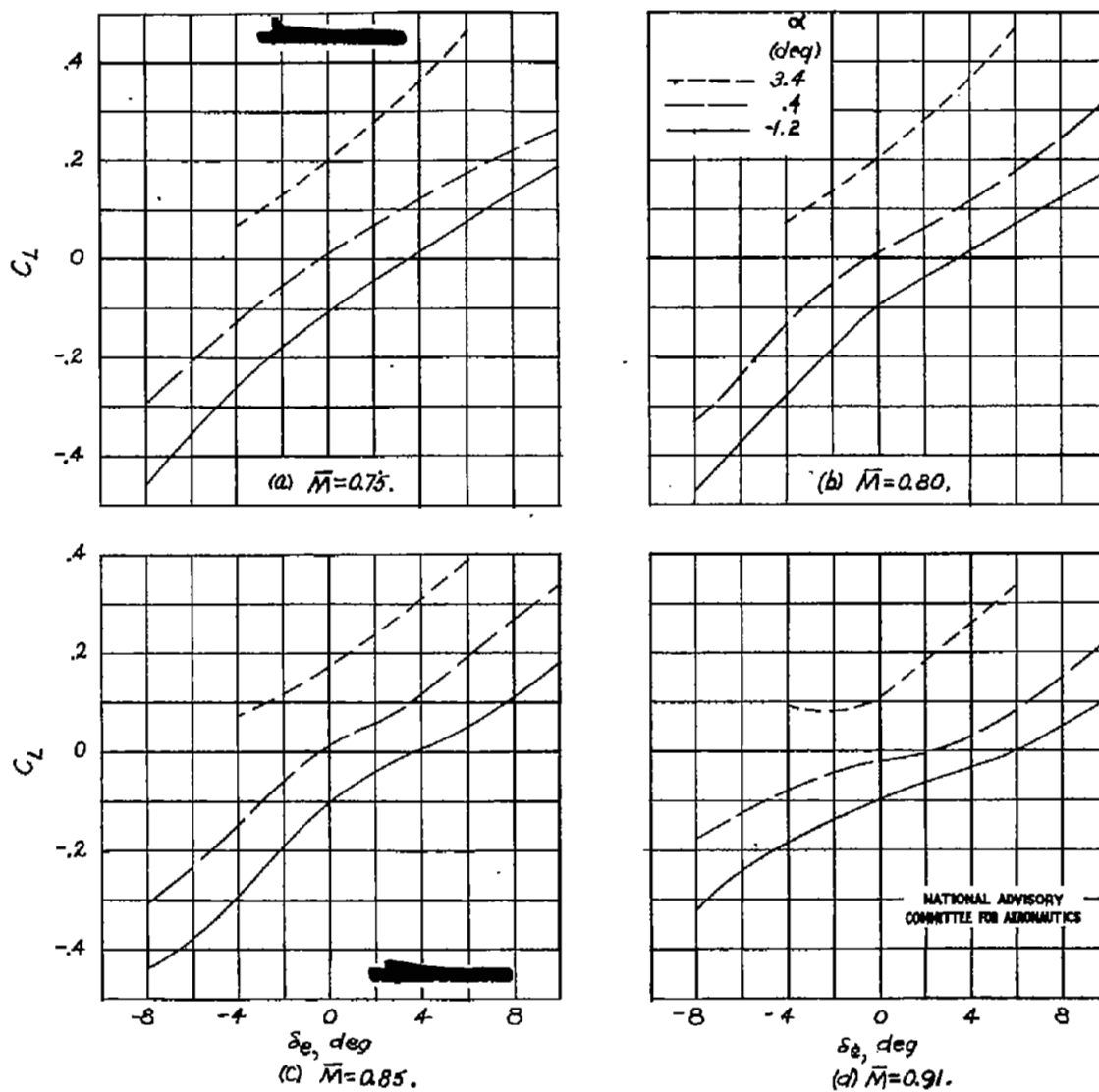
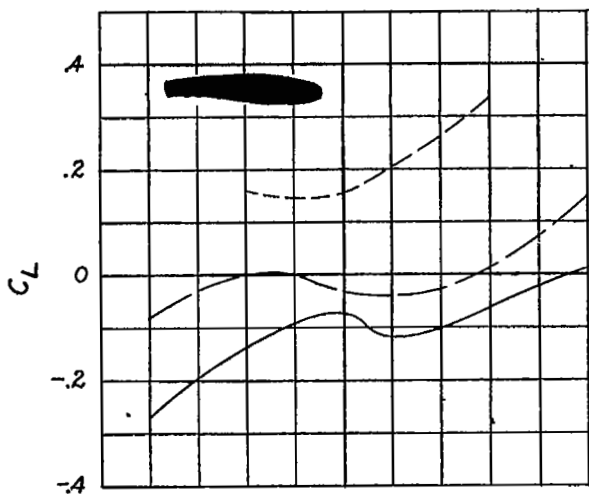
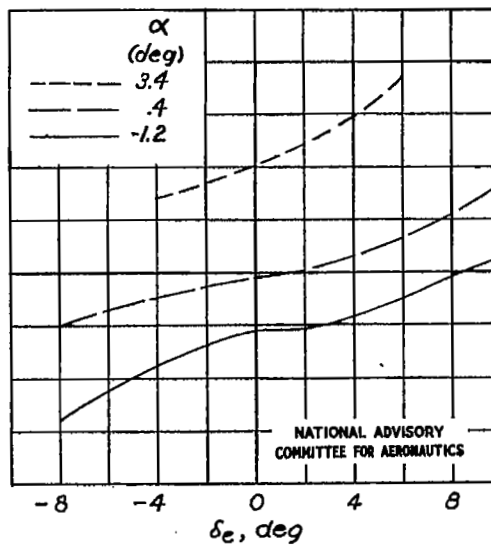


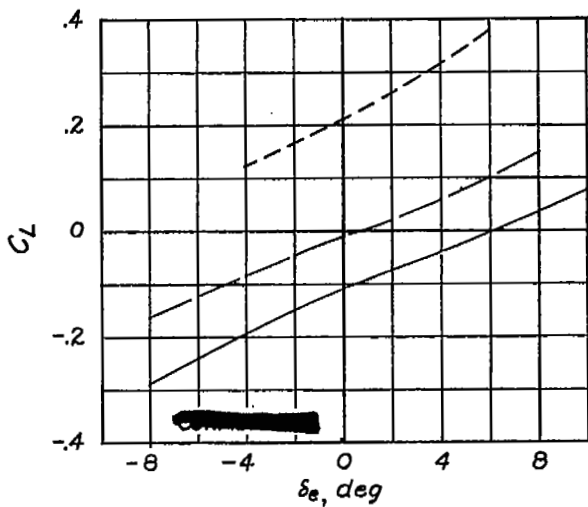
Figure 8.- Variation of lift coefficient with elevator deflection for three angles of attack and for several Mach numbers.



(e) $\bar{M} = 0.96$.

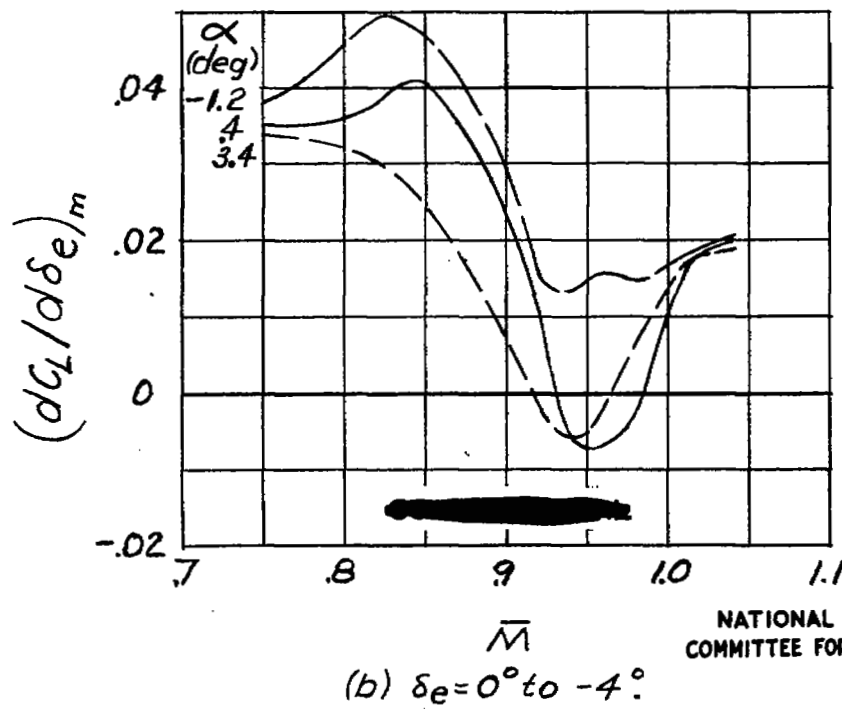
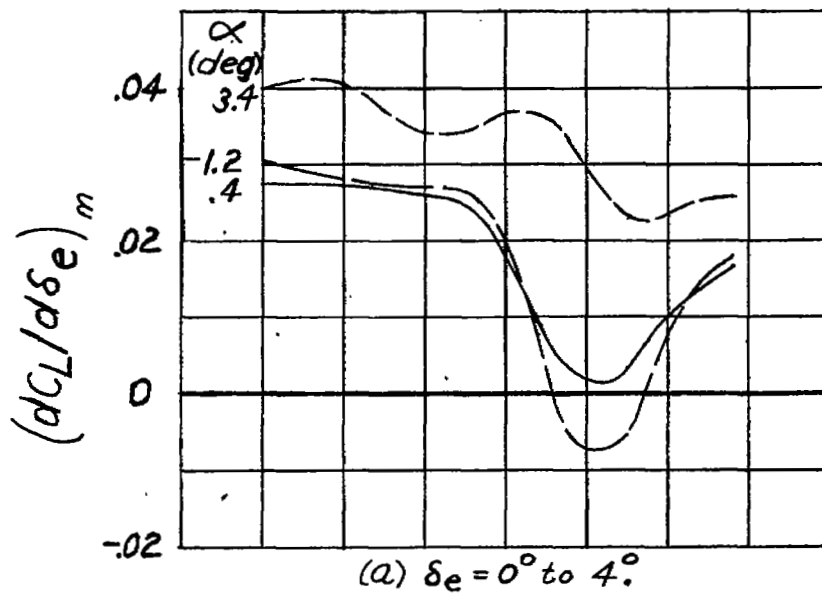


(f) $\bar{M} = 1.00$.



(g) $\bar{M} = 1.04$.

Figure 8.- Concluded.



NATIONAL ADVISORY
COMMITTEE FOR AERONAUTICS

Figure 9.- Elevator effectiveness over the deflection range 0° to 4° and 0° to -4° for three angles of attack.

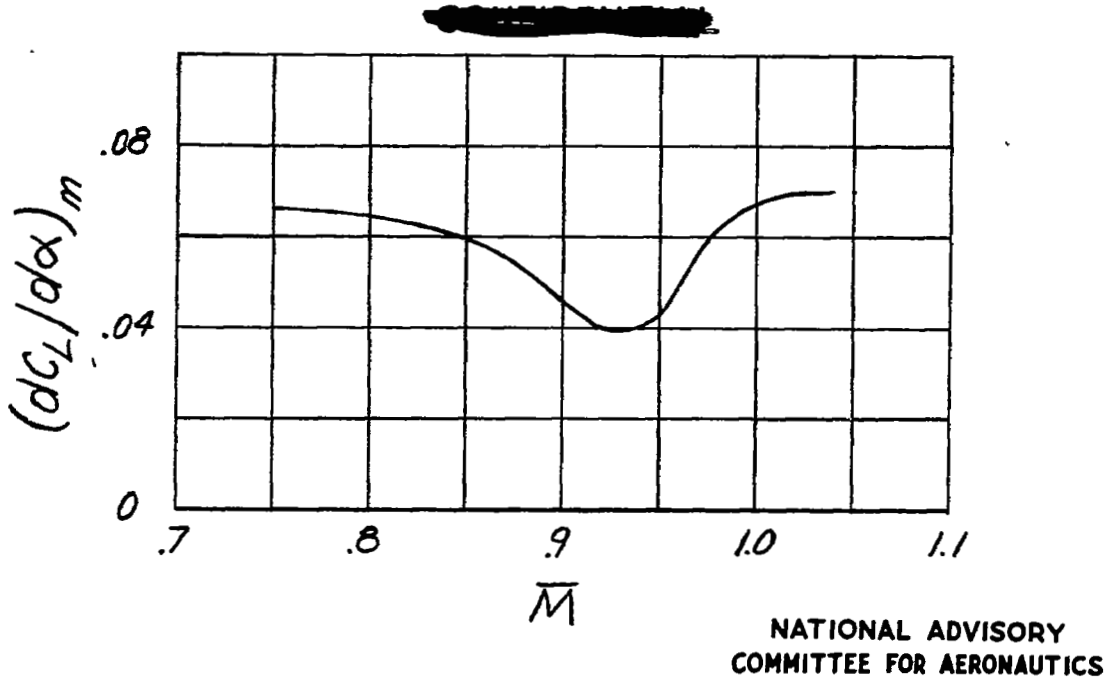


Figure 10.- Stabilizer effectiveness. Angle of attack, -1.2° to 3.4° ; elevator neutral.

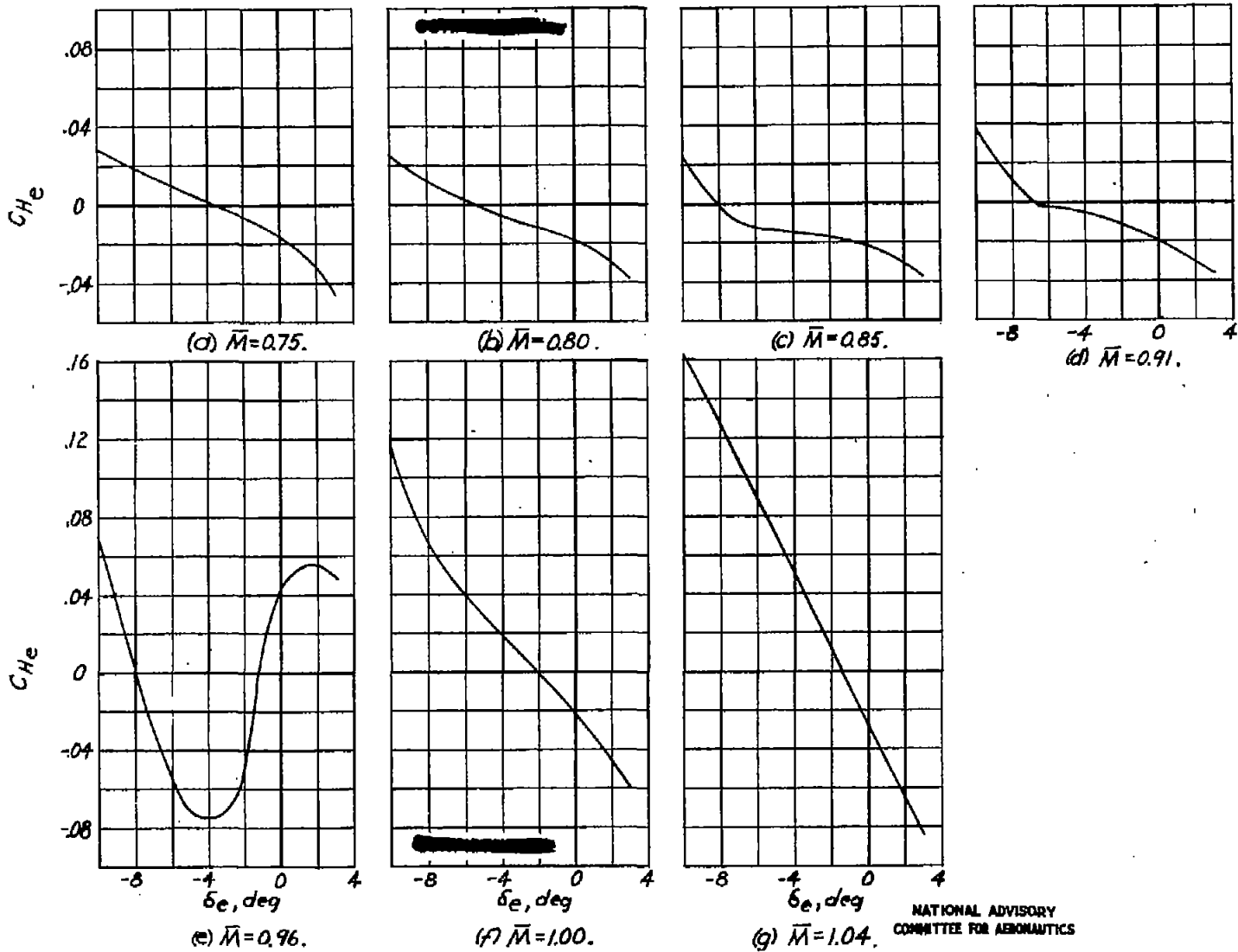


Figure 11.- Variation of elevator hinge-moment coefficient with elevator deflection for an angle of attack of 0.4° and for several Mach numbers.

NATIONAL ADVISORY
COMMITTEE FOR AERONAUTICS

Model	A	$(t/c)_m$	Elevator	c_e/c	R
Horizontal tail of a fighter airplane (wing flow)	3.99	0.10	Bulged, unsealed	0.33	$0.67 \text{ to } 0.84 \times 10^6$
Typical high-speed-bomber horizontal tail (tunnel)	4.01	0.08	Straight contour, sealed	0.30	$1.83 \text{ to } 1.94 \times 10^6$

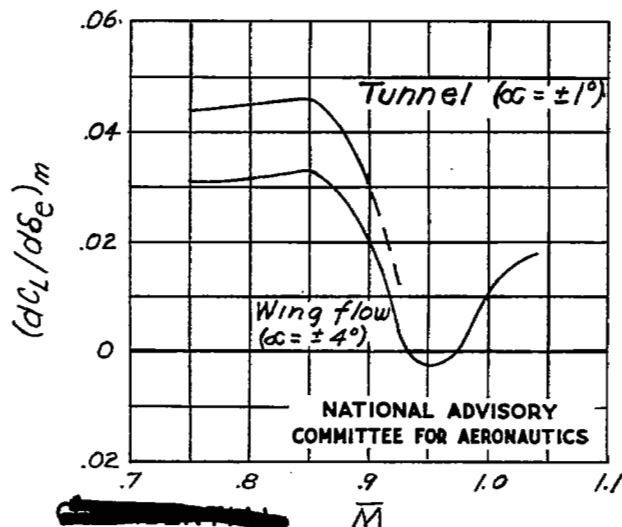
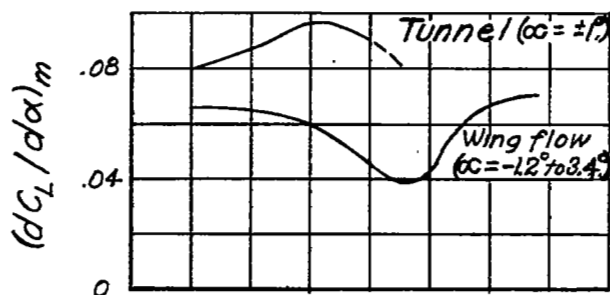


Figure 12.- Variation with Mach number of elevator and stabilizer effectiveness from wing-flow tests of a horizontal-tail model of a fighter airplane and wind-tunnel tests of a typical high-speed-bomber horizontal tail.

NASA Technical Library



3 1176 01436 3387